Cluster-CMSS: A Cluster-Based Coordinated Spectrum Sensing in Geographically Dispersed Mobile Cognitive Radio Networks

Behzad Shahrasbi, *Member, IEEE*, Nazanin Rahnavard, *Member, IEEE*, and Azadeh Vosoughi, *Senior Member, IEEE*

***Abstract*—A coordinated multiband spectrum sensing (CMSS) policy for mobile and geographically dispersed cognitive radio networks (CRNs), referred to as cluster-CMSS, is proposed. The goal is to detect the spectrum holes and to assign each secondary user (SU) a sensing channel with the maximum probability of being empty. In geographically dispersed CRNs, channel availability varies over the space, and this makes the sensing outcomes and sensing assignments location dependent. However, if the SUs are not equipped with location-finding technologies, fusing the sensing outcomes to find the optimal spectrum sensing assignments for the next sensing time becomes challenging for the base station (BS). To tackle this problem, we introduce a metric solely based on the sensing outcomes of SUs. Using this metric, along with a low-complexity clustering algorithm, enables the BS to efficiently divide the network into clusters. Further, we present an adaptive learning algorithm, to learn the dynamic behavior of channel occupancy in the primary network. The proposed learning algorithm considers SUs mobility model to determine the optimal learning window. To determine the sensing assignments, the BS performs a graph-theory-based coordinated multiband spectrum sensing within each cluster. Specifically, a weighted bipartite matching is employed. We have shown that cluster-CMSS significantly increases the spectrum opportunity discovery ratio for SUs at the cost of a slight increase in the energy consumption associated with spectrum sensing.**

***Index Terms*—Clustering, cognitive radio (CR), mobility, random waypoint, spectrum sensing, wideband communication.**

I. Introduction

COGNITIVE radio (CR) is a promising solution to alleviate today's spectrum deficiency caused by an increased demand for wireless technologies [1]. The CR paradigm allows a new type of users called unlicensed users or secondary users (SUs) to coexist with the licensed users or primary users (PUs). The SUs are allowed to access the spectrum provided that they do not interfere with the PUs. The underutilized spectrum bands that can be used by the SUs are called spectrum holes [2]. The availability of spectrum holes for each SU varies in both *time* and *space* since the PUs' presence is dispersed both in temporal and spatial domains. An ideal CR is able to efficiently detect and utilize all spectrum holes. Due to the dynamic behavior of PUs, SUs should constantly be aware of the occupancy status of multiple narrow bands or channels of spectrum (a.k.a., wideband spectrum sensing). However, implementing wideband spectrum sensing requires considerable amount of time or complex hardware [3] to obtain a fairly good estimate of the entire spectrum. This lengthy estimation will significantly reduce SUs opportunity to transmit their own data [4].

In this paper, we propose a spectrum sensing policy for geographically dispersed networks that do not require location information of the SUs. Our proposed method is referred to as *cluster-based coordinated multiband spectrum sensing* (cluster-CMSS). We assume SUs are mobile and can communicate with a central node or *base station* (BS). This is a complex problem with several challenges including limited ability of SUs in sensing the spectrum, geographically dispersed SU distribution, dynamic PU activity, and inaccurate sensing. To the best of our knowledge, this is the first attempt that addresses all these challenges simultaneously.

The main contribution of this paper is addressing coordinated spectrum sensing problem in the geographically dispersed and mobile cognitive radio networks (CRNs). The novelty of the proposed framework is threefold. First, we propose a novel *metric* that allows us to group the SUs based on the similarity of spectrum holes that they can find. Second, we propose a learning algorithm for estimating the PU's dynamic based on the mobility of SUs. Third, we propose a novel energy-efficient and fast coordinated spectrum sensing policy that maximizes the channel discovery ratio for SUs.

The rest of this paper is organized as follows. In Section II, the related work on CMSS, clustering of SUs in geographically dispersed networks, and mobility in CRNs are discussed. In Section III, we describe the CMSS problem, the model of SUs' operation, and the PUs' activities model. Section IV describes our proposed Cluster-CMSS policy for the geographically dispersed and mobile CRNs. In Section V, we find the probabilities of misdetection and false alarm and also the energy cost of our policy. In Section VI, we provide the simulation results and discuss our findings. Finally, Section VII concludes this paper.

Manuscript received September 3, 2015; revised October 3, 2016; accepted May 12, 2016. Date of publication November 22, 2016; date of current version July 14, 2017. This work was supported by the National Science Foundation under Grant ECCS-1418710 and Grant CCF-1439182. The review of this paper was coordinated by Dr. X. Huang.

The authors are with the Department of Electrical Engineering and Computer Science, University of Central Florida, Orlando, FL 32816 USA (e-mail: behzad.shahrasbi@knights.ucf.edu; nazanin@eecs.ucf.edu; azadeh@ucf.edu).

Color versions of one or more of the figures in this paper are available online at http://ieeexplore.ieee.org.

Digital Object Identifier 10.1109/TVT.2016.2631595

II. Related Work

Spectrum sensing in CRNs is a very well-studied topic in the literature. However, some of its aspects received more attention compared to others. For example many studies have extensively covered issues such as *cooperation* among SUs to reliably detect the spectrum holes [5], [6] or spectrum sensing employing energy detectors [7], improved energy detectors [8], and cyclostationary features [3]. On the other hand, the networks that include mobility or geographically dispersed SUs are underinvestigated.

The problem of spectrum opportunity discovery when the BS is aware of SUs locations is studied in [5]. The authors quantified the gain that is achieved by simultaneously employing both spatial and temporal spectrum holes versus employing them individually. In [6], the problem of joint spatial and temporal spectrum opportunity discovery for a case of single PU band is considered.

In [9], the joint problem of spectrum sensing and access in geographically dispersed CRNs are formulated in the form of a restless multiarmed bandit problem and the bounds for the regret of the proposed policies are found. In [10], an iterative Hungarian algorithm is proposed to find the sensing assignment that minimizes the probability of misdetection. This algorithm assigns SUs to sense different channels assuming that the channel availability is consistent among all the SUs. In [11], a machine-learning-aided spectrum sensing policy is proposed, in which each SU is assigned to sense the channel that provides the SU with the highest throughput.

In all the mentioned studies, it is assumed that SUs are static. Given that mobility significantly affects the performance of spectrum sensing [12], it is of great importance to consider the effect of mobility in learning the PU's activity and also spectrum sensing assignment. However, in the context of spectrum sensing for CR this problem has not received much attention. Most of the previous works on mobile CRNs are dealing with routing or connectivity issues [13]. The work in [12] is among the first that shows SU's mobility increases spatio-temporal diversity in the received PU's signal and improves the sensing performance. In [14], a mobility-aware cluster-based cooperative spectrum sensing approach has been proposed. The authors have shown that in case of cooperation, the mobility-aware clustering improves the channel discovery ratio and the throughput.

In [15], we proposed a cluster-based coordinated spectrum sensing algorithm that employs the Kullback–Leibler (KL) divergence between the previous sensing results of SU to form the clusters. After the clusters are formed, SUs within each cluster perform the CMSS algorithm. In [16], a noncentralized clustering approach is employed to cluster the SUs based on their channel sensing outcomes. In [16], it is assumed that SUs already have the availability information of all channels either through sensing or a databases query and forms the clusters such that the cluster members have maximum idle PU channels in common. In [17] and [18], the SUs are grouped into clusters and for each cluster the best channel to sense is determined. In these papers, all the members of a cluster sense the same channel, which is in contrast to our approach. Additionally in [19] and [16], clustering is employed to reduce the network management traffic.

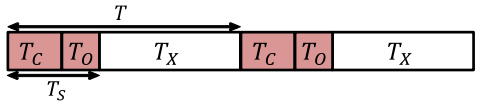

Fig. 1. Frame structure of an SU's operation in a CRN depicting two consecutive time frames. During the sensing time T_S, all SUs cease their transmissions.

Although different aspects of spectrum sensing in CRs have been studied individually, to the best of our knowledge, this is the first study that addresses the cluster-based coordinated multiband spectrum sensing for mobile SUs.

III. System Model

The entire spectrum of interest is divided into M *orthogonal frequency subbands* or PU channels each with bandwidth W. The SU network consists of N mobile wireless terminals (or simply SUs) and a stationary BS. Each SU is equipped with a *single antenna* and can perform either sensing or transmission at a time. The RF front end of SUs employs *energy detectors* and can reliably sense only one PU channel per sensing. For now, we consider the ideal sensing case (in which probabilities of misdetection and false alarm are both zero) while describing our proposed policy. Later, in Section V, we consider the nonideal sensing scenarios. In addition, similar to many other studies (e.g., [17]), we assume a dedicated common control channel exists between the SUs and the BS and all SUs can directly communicate with the BS. The SUs move based on a *random waypoint* mobility model. According to this model, SUs movement occurs in *epochs*. At the beginning of each epoch, an SU independently chooses a destination in the network (a *waypoint*) uniformly at random and starts moving toward that destination at a constant velocity, which is chosen uniformly at random from the interval $[v_{\min}, v_{\max}]$. When the SU reaches its destination, it pauses for t_p seconds until it starts a new epoch following the same rule. We represent such mobility model with RWP$(v_{\min}, v_{\max}, t_p)$. It is worth nothing that epochs are not synchronized among different SUs. In this paper, we assume $v_{\max}$ is small enough that we can safely ignore the carrier offset caused by Doppler effect.

The primary network consists of N_p PUs distributed uniformly at random. Each PU operates in some of the M channels or subbands. As in [20], to model each PU's activity at each channel, we adopt an independent two-state Markov process alternating between the busy (B) and empty (E) states. Let $\alpha_{l,i}$ and $\beta_{l,i}$ be the probabilities that channel i of PU l switches its state from B to E and from E to B, respectively, for $i = 1, 2, \ldots, M$ and $l = 1, 2, \ldots, N_p$. The utilization of channel i of PU l is given by $\lambda_{l,i} = \frac{\beta_{l,i}}{\beta_{l,i}+\alpha_{l,i}}$ [20].

A. Frame Structure of CRNs

The SUs are assumed to be synchronized and operate in time on a frame-by-frame structure as in [20]. The frame structure of a CRN, as shown in Fig. 1, includes a sensing time T_S and a transmission time T_X that adds up to the total frame time T. During sensing time (T_S) all SUs cease their transmission, perform spectrum sensing for T_C seconds, and report the sensing results on a dedicated common control channel to the BS for

T_O seconds. In the IEEE 802.22 standard T is set at about a few hundred milliseconds [20].

B. SU's Belief Vector

In the geographically dispersed SU network, PU's transmission can only be detected within a specific area. Outside that area, an SU can use the same channel for its transmissions (*frequency reuse*). This implies that PU channels' availability information is *inconsistent* in geographically dispersed SUs. Due to limited sensing capability of the SUs the state of every PU at every SU location cannot be observed. However, each SU may infer the state of PUs from the observation history. To this aim, let us define the *belief vector* $\boldsymbol{x}_j(t) \triangleq [x_{j,1}(t), \ldots, x_{j,M}(t)]$, where $x_{j,i}(t)$ is the probability that SU j finds channel i empty at time t (whether or not it actually senses it). Let $a_j(t)$ denote the channel that SU j senses at time t. Moreover, let $S_{a_j(t)}(t) \in \{B, E\}$ be the status of the observed channel by SU j at time t.

The belief vector for SU j at time $t+1$ is obtained as follows:

$$x_{j,i}(t+1) = \begin{cases} 1 - \bar{\beta}_{j,i}(t), & a_j(t) = i, S_{a_j(t)} = E \\ \bar{\alpha}_{j,i}(t), & a_j(t) = i, S_{a_j(t)} = B \\ x_{j,i}(t)(1 - \bar{\beta}_{j,i}(t)) & \\ \quad + (1 - x_{j,i}(t))\bar{\alpha}_{j,i}(t) & a_j(t) \neq i. \end{cases} \tag{1}$$

In (1), $\bar{\alpha}_{j,i}(t)$ and $\bar{\beta}_{j,i}(t)$ are the state transition probabilities of channel i from the perspective of SU j at time t. While $\alpha_{l,i}$ and $\beta_{l,i}$ are deified for every PU, $\bar{\alpha}_{j,i}$ and $\bar{\beta}_{j,i}$ are defined from SUs' standpoint. Therefore, due to mobility of SUs, $\bar{\alpha}_{j,i}(t)$ and $\bar{\beta}_{j,i}(t)$ are constantly changing. In addition, finding $\bar{\alpha}_{j,i}(t)$ and $\bar{\beta}_{j,i}(t)$ in terms of $\alpha_{l,i}$ and $\beta_{l,i}$, respectively, is not possible due to the lack of location information. After each SU completes the sensing at time t, it transmits the sensing decision to the BS and then BS calculates the beliefs based on (1) and stores $\boldsymbol{x}_j(t+1)$ for all $j = 1, 2, \ldots, N$. Consequently, the BS determines the sensing policy $\boldsymbol{a}(t+1) \triangleq [a_1(t+1), \ldots, a_N(t+1)]$, where $a_j(t+1)$ determines the channel that SU j senses at time $t+1$.

IV. Cluster-Coordinated Multiband Spectrum Sensing

In this section, we explain our proposed policy, referred to as cluster-CMSS, to find the optimal sensing policy. First, we consider a scenario where the PU's dynamic (i.e., $\alpha_{l,i}$ and $\beta_{l,i}$ for all $i = 1, 2, \ldots, M$ and $l = 1, 2, \ldots, N_p$) is known. Later in this section, we consider a scenario where the dynamic of the PU activity is learned.

A. Cluster-CMSS Policy With Known PU Dynamic

When $\bar{\alpha}_{j,i}(t)$ and $\bar{\beta}_{j,i}(t)$ for all $i = 1, 2, \ldots, M$ and $j = 1, 2, \ldots, N$ are known, the BS can update the belief vectors using (1). The cluster-CMSS algorithm is initialized to $\boldsymbol{x}_j(1) = [\frac{1}{2}, \frac{1}{2}, \ldots, \frac{1}{2}]^T$ for all $j = 1, 2, \ldots, N$. Therefore, the BS assigns a channel to each SU uniformly at random. At the beginning of the consequent time frames, the BS, after receiving the sensing results from the SUs, performs the following steps. The BS updates the belief vectors for all SUs, based on which the SUs are partitioned into several clusters (details will be discussed in Section IV-C). For every cluster, the BS determines the unique channels to be sensed in the next time frame by performing a one-to-one matching algorithm (details will be discussed in Section IV-D) between the members of that cluster and the channels. Algorithm 1represents the pseudo code of the steps taken at the beginning of each frame. The flowchart of our proposed policy is given in Fig. 2. The tasks during T_S at the BS and SUs are depicted in right and left boxes, respectively. To measure the overall performance of the proposed policy, we define average *spectrum opportunity discovery ratio* $\bar{R}_s$. This is the ratio of the average number of *unique* spectrum holes discovered per time frame $\bar{n}_u$ to the total number of sensing attempts per time frame N. This can be evaluated by averaging the instantaneous ratio of these parameters over time (i.e., $\bar{n}_u = E[n_u(t)]$). At time t, the number of unique spectrum holes can be obtained by subtracting the number of duplicate sensed spectrum holes $n_d(t)$ from the total number of successful sensing attempts $n_s(t)$. If two or more SUs are located within transmission range of each other and they sense the same channel empty in one time frame, one of these sensing attempts is considered unique and the rest are duplicate spectrum holes. Therefore, $\bar{R}_s$ is obtained as follows:

$$\bar{R}_s = \frac{\bar{n}_u}{N} = \frac{\bar{n}_s - \bar{n}_d}{N} = \frac{E[n_s(t)] - E[n_d(t)]}{N}. \tag{2}$$

Algorithm 1: The proposed cluster-CMSS algorithm at the beginning of frame t.

1: SUs sense the assigned channels.
2: The BS receives the sensing results (B or E) from SUs.
3: The BS determines the belief vectors $\boldsymbol{x}_j(t+1)$ for all $j = 1, 2, \ldots, N$ (1).
4: The BS partitions SUs into clusters (Section IV-C).
5: The BS performs bipartite matching (Section IV-D) within each cluster and assigns each SU a channel to sense in the next time frame (some SUs will remain inactive).
6: The BS transmits the channel access permissions and the ID of the channel that each SU has to sense at frame $t+1$.

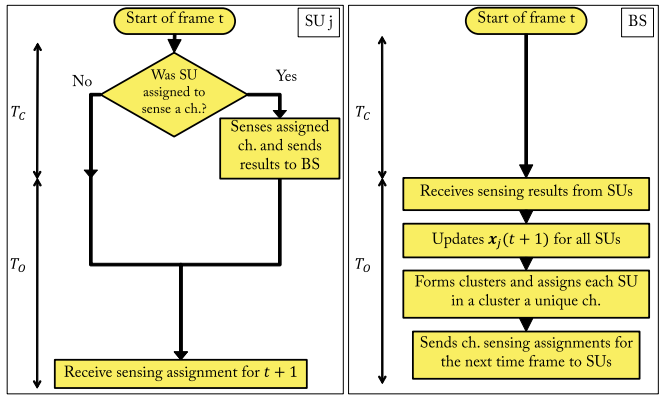

Fig. 2. Flowcharts of the proposed cluster-CMSS policy. The tasks during T_S at the BS and SUs are depicted in right and left boxes, respectively.

In the rest of this section, we separately describe the building blocks of our proposed cluster-CMSS policy. It should be noted that Algorithm 1is proposed under the assumption that spectrum sensing is ideal. For nonideal channel sensing scenarios, developing a spectrum sensing policy would be more challenging in the mobile-network scenarios. Hence, the estimates of probabilities of false alarm and detection should be available and included in the policy.

B. Learning the PU Dynamic

In most real-world scenarios, the dynamic of the PUs arrival and departure are *a priori* unknown and are difficult to estimate accurately. Therefore, the BS needs to learn them on the fly. A simple and practical method of learning PU's dynamic is by recording the sample means of $\bar{\alpha}_{j,i}(t)$ and $\bar{\beta}_{j,i}(t)$ for all $i = 1, 2, \ldots, M$ and $j = 1, 2, \ldots, N$ [21]. In other words, the BS determines the number of times that each SU observes a certain channel has changed its state from empty to busy and vice versa. Therefore, the estimated values of these parameters $\hat{\alpha}_{j,i}(t)$ and $\hat{\beta}_{j,i}(t)$ will be used in (1). To estimate these parameters, we define a *learning window* with length T_l time frames in which the number of state transitions is counted. When the SUs are static, increasing the length of the learning window will add to the accuracy of the parameter estimations. However, in mobile SUs scenarios having a lengthy learning window reduces the accuracy of parameter estimation because of the SUs movements. In the following, we determine the optimal length of learning window under random waypoint mobility model for SUs.

We propose to choose the length of the learning window equal to the average time it takes a mobile SU to move out of an active PU's range. In other words, the previous sensing results of an SU that are older than this average time are no longer useful in determining the PU's dynamic. The following theorem provides tight upper and lower bounds for the average time it takes for an SU to move out of an active PU's range.

Theorem 1. Assume a circle with radius R entirely located at random inside an area A with a rectangular shape. Given an SU exists within the boundaries of this circle. The average time it takes for this SU, which moves based on the random waypoint model RWP$(v_{\min}, v_{\max}, t_p)$, that remains inside the circle is denoted by T_r and is bounded as follows:

$$\frac{2}{v_{\min}+v_{\max}}\left(\frac{P_{\text{in}}}{1-P_{\text{in}}}\frac{128R}{45\pi}+1\right)+\frac{P_{\text{in}}}{1-P_{\text{in}}}t_p \le T_r \le \frac{2}{v_{\min}+v_{\max}}\left(\frac{P_{\text{in}}}{1-P_{\text{in}}}\frac{128R}{45\pi}+\frac{4}{3}\right)+\frac{P_{\text{in}}}{1-P_{\text{in}}}t_p \quad (3)$$

where P_{in} is the probability that a waypoint falls inside the circle and is given by $P_{\text{in}} = \frac{\pi R^2}{A}$.

Proof. See Appendix A. ■

Using Theorem 1, we set the length of the learning window to be the closest multiple of T to the midpoint of the upper and lower bounds given in (3). That is

$$T_l = \text{rnd}\left(\frac{2}{(v_{\min}+v_{\max})T}\left(\frac{P_{\text{in}}}{1-P_{\text{in}}}\frac{128R}{45\pi}+\frac{7}{6}\right)+\frac{P_{\text{in}}}{1-P_{\text{in}}}t_p\right). \quad (4)$$

In (4), the function rnd(.) rounds its argument to the nearest integer. Clearly, when SUs are static ($v_{\max} = v_{\min} = 0$), both the upper and the lower bounds of T_l reaches ∞, which means the length of learning window can grow very large. In other words, we can use all of previous sensing results to estimate the channel parameters. Given the length of the learning window T_l the BS can calculate the average number of state transitions that it has observed per channel for each SU during the learning window. For instance $\hat{\alpha}_{j,i}(t)$ is determined by dividing the number of times SU j observes channel i changed its state from B to E to the number of times SU j has observed the state of channel i to be in B state during past T_l sensing attempts. The value of $\hat{\beta}_{j,i}(t)$ is calculated in the same way for all SUs and PU channels. It is worth noting that in some cases, specially when the velocity of SUs is high, an SU may not observe one or more channels during T_l. In those cases, the estimated parameters from previous time frame is used.

C. The Sensing-Based Clustering

In the geographically dispersed networks, clustering allows frequency reuse and more efficient spectrum sensing. By grouping the nodes that share the same set of spectrum holes, the BS can coordinate sensing assignment among members of every cluster. In the lack of SU's location information, we propose to use the *sensing results of SUs* as a *clustering metric*. We define the distance between two SUs based on the distance between their belief vectors. More specifically, we define the distance D_x between any two SUs as the KL divergence between beliefs of those SUs. In other words, the distance is measured by the divergence in the beliefs of SUs j_1 and SU j_2 and is defined as follows:

$$D_x(j_1, j_2) \triangleq D_{\text{KL}}(\boldsymbol{x}_{j_1}(t)\|\boldsymbol{x}_{j_2}(t)) + D_{\text{KL}}(\boldsymbol{x}_{j_2}(t)\|\boldsymbol{x}_{j_1}(t)) \quad (5)$$

where $D_{\text{KL}}(\boldsymbol{x}_{j_1}(t)\|\boldsymbol{x}_{j_2}(t)) \triangleq \sum_{i=1}^{m} x_{j_1,i}(t)\log\frac{x_{j_1,i}(t)}{x_{j_2,i}(t)}$. If two SUs experience exactly the same set of observations on PUs' channels, they will have the same beliefs on PU's channels and the KL distance between them will be zero. Similarly, SUs with different PU's channel sensing experiences will have diverged beliefs and consequently greater distances.

Various clustering algorithms have been proposed in the literature for different purposes in CRNs. In our case, we are interested in a clustering algorithm that provides *hard partitioning*, has *low complexity*, and operates without the prior knowledge on PU's dynamic. To meet these requirements and to cluster SUs, we integrate our proposed *sensing distance* metric [defined in (5)] into the k-means clustering method. Since the number of clusters is not known *a priori,* we use the *elbow method* to determine the number of clusters. Accordingly, we start with $k = 1$ cluster and find point-to-centroid distance variance within the

Algorithm 2: The intracluster CMSS algorithm at frame t.

1: **for** every cluster **do**
2: Calculate the weights according to $w_{j,i}(t) = \frac{1}{x_{j,i}(t)+\epsilon}$ for all $j \in \{1, \ldots, N_k\}$ and $i \in \{1, \ldots, M\}$.
3: Run the minimum-weight *Hungarian* algorithm [23].
4: **end for**
5: Transmit obtained channel sensing assignment results to SUs.

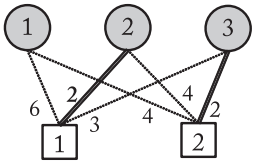

Fig. 3. Example of CMSS within a cluster using bipartite matching.

cluster. By increasing k, point-to-centroid variance decreases within the cluster. However, there exists a k, k_{opt}, beyond which increasing the number of cluster will only improve the variance marginally. This point is called the elbow point [22].

D. Coordinated Spectrum Sensing Within Clusters Using Bipartite Matching

In this section, we describe the mapping of the CMSS problem onto a bipartite matching problem. After the BS clusters the SUs, it assigns each SU within each cluster a unique channel to sense. The goal is to assign each SU to sense the channel it believes to have the highest probability of being empty. For each cluster, the BS solves this problem by finding a *minimum-weight matching* on a bipartite graph that is constructed as follows.

The vertices of one side of the graph correspond to the SUs in a cluster (i.e., N_k vertices) and the vertices of the other side of the graph correspond to the PU channels (i.e., M vertices). An edge exists between any two vertices from each side of this bipartite graph with a positive weight (see Fig. 3). We inversely relate $w_{j,i}(t)$, the weight of the edge connecting SU j to channel i, to $x_{j,i}(t)$, the belief SU j on channel i. Therefore, the greater the $x_{j,i}(t)$, the smaller the weight of edge between channel i and SU j. The weights of each edge is set as $w_{j,i}(t) = \frac{1}{x_{j,i}(t)+\epsilon}$, where ϵ is a very small constant to avoid unbounded weights. Using this strategy, we find the minimum-weight allocation that corresponds to maximizing the probability of finding an empty channel for each cluster member. We employ the well-known Hungarian algorithm [23] to solve the minimum-weight matching problem. Algorithm 2 represents the proposed intraclustering assignment. Fig. 3 depicts an example of CMSS within a cluster using bipartite matching. In this example, $M = 3$ (circles), for this cluster $N_k = 2$ (squares), and the weight of each edge is represented by its corresponding edge. The double-lined edges represent the minimum weight matching and the dashed edges represent the unmatched edges. Based on this matching, SU 1 and SU 2 will sense channels 2 and 3, respectively.

V. Performance Evaluation of Cluster-Coordinated Multiband Spectrum Sensing

In this section, we study the performance of our proposed cluster-CMSS algorithm. Suppose $A(t)$ is the set of SUs that has been assigned by the BS to perform spectrum sensing at time frame t and $|A(t)|$ be the cardinality of $A(t)$. We find the probabilities of misdetection $P_m^j(t)$ and false alarm $P_f^j(t)$ for all $j \in A(t)$ under the AWGN, Rayleigh, Rician, and Nakagami-m channel models. The average probabilities of misdetection $Q_m(t)$ and false alarm $Q_f(t)$ are given by

$$Q_m(t) = \frac{1}{|A(t)|} \sum_{j \in A(t)} P_m^j(t) \tag{6}$$

$$Q_f(t) = \frac{1}{|A(t)|} \sum_{j \in A(t)} P_f^j(t). \tag{7}$$

The SUs that are not assigned to sense any channel do not contribute to the $Q_m(t)$ and $Q_f(t)$. In the following, for the brevity of expressions we omit variable t from all formulas.

A. Misdetection and False Alarm Probabilities Over AWGN Channels

Suppose γ_j is the received SNR at SU j. A closed-form expression for the probabilities of misdetection P_m^j and false alarm P_f^j of SU j over the AWGN channel are as follows [24]:

$$P_f^j = \frac{\Gamma(T_C W, \frac{\delta}{2})}{\Gamma(T_C W)} \tag{8}$$

$$P_m^j = 1 - Q_{T_C W}(\sqrt{2\gamma_j}\sqrt{\delta}) \tag{9}$$

where δ is the decision threshold, $\Gamma(.)$ is the gamma function, $\Gamma(.,.)$ is the incomplete gamma function, and $Q_{\square}(.,.)$ is the generalized Marcum Q-function [24]. Without loss of generality, we choose the value of T_C such that $T_C W$ is restricted to be an integer. The value of T_C can be determined such that it keeps P_f^j and P_m^j below predefined thresholds for all $j \in \{1, \ldots, N\}$.

B. Misdetection and False Alarm Probabilities Over Rayleigh, Rician, and Nakagami-m Channels

In practical networks, the spectrum sensing quality might be adversely affected by fading. In this section, we briefly consider the scenarios in which the SNR of the sensed signal at SUs follows Rayleigh, Rician, and Nakagami-m distributions. Rician model represents the scenarios in which SUs receive the PU signal from several different paths, with one direct path that is stronger than the others. Rician factor K is the ratio between the power received from the direct path and the power received from other scattered paths [25]. Parameter K is an indicator of the severity of the fading [26]. A smaller K indicates a sever fading. Rayleigh model is suitable for scenarios where the direct path does not exist (severe fading). Therefore, the Rayleigh fading channel is a special case of Rician fading channel with $K = 0$. For $K = \infty$, the Rician channel boils down to AWGN channel (with no fading).

In addition, Nakagami-m distribution has gained substantial application in modeling fading channels because of the good

fit to the empirical data [27]. The parameter m determines the severity of the fading channel. The smaller values of parameter represent more severe fading condition. For instance $m = 1$ corresponds to Rayleigh fading and $m = \infty$ corresponds to AWGN channel. In addition, Nakagami-m model reduces to Rician with parameter K for $m = \frac{(K+1)^2}{2K+1}$ [26].

Clearly, P_f^j remains the same under the fading scenario because P_f^j is independent of the received SNR. In the case of Rician channel, the received SNR γ_j is a random variable that follows Rician distribution. The PDF of γ_j for all $\gamma_j > 0$ is given by [24]

$$f(\gamma_j) = \frac{K+1}{\overline{\gamma_j}} \exp\left(-K - \frac{(K+1)\gamma_j}{\overline{\gamma_j}}\right) \times I_0\left(2\sqrt{\frac{K(K+1)\gamma_j}{\overline{\gamma_j}}}\right) \tag{10}$$

where $\overline{\gamma_j}$ is the average SNR at SU j and can be estimated as described in [25], and $I_0(.)$ is the zeroth-order modified Bessel function of the first kind.

The probability of misdetection $P^j_{m\,\text{Rice}}$ can be obtained by averaging (9) over the Rician distribution in (10). A closed-form expression is given in [24] for special case of $T_C W = 1$

$${P_m}^j{}_{\text{Rice}}|_{T_C W=1} = 1 - Q_{T_C W=1}\left(\sqrt{\frac{2K\overline{\gamma_j}}{K+1+\overline{\gamma_j}}}\sqrt{\frac{\delta(K+1)}{K+1+\overline{\gamma_j}}}\right). \tag{11}$$

For $K = 0$, this expression reduces to Rayleigh fading [24].

In the case of Nakagami-m model, the received SNR γ_j is a random variable that follows Nakagami-m distribution. The PDF of γ_j, for all $\gamma_j \geq 0$, is given by [24]

$$f(\gamma_j) = \frac{1}{\Gamma(m)}\left(\frac{m}{\overline{\gamma_j}}\right)^m \gamma_j^{m-1} \exp\left(-\frac{m}{\overline{\gamma_j}}\gamma_j\right) \tag{12}$$

where $\overline{\gamma}_j$ is the average received SNR at SU j. The probability of misdetection $P^j_{m\,\text{Nak}}$ can be obtained by averaging (9) over the Nakagami-m distribution in (12). A closed-form expression is given in [24]

$${P_m}^j{}_{\text{Nak}} = 1 - \alpha\left[G_1 + \beta\sum_{n=1}^{\text{TW}-1}\frac{(\delta/2)^2}{2(n!)}{}_1F_1 \times \left(m; n+1; \frac{\delta}{2}\frac{\overline{\gamma_j}}{(m+\overline{\gamma_j})}\right)\right] \tag{13}$$

where $\alpha = \frac{1}{\Gamma(m)2^{m-1}}(\frac{m}{\overline{\gamma_j}})^m$, $\beta = \Gamma(m)(\frac{2\overline{\gamma_j}}{m+\overline{\gamma_j}})^m \exp^{-\delta/2}$, and ${}_1F_1(.;.;.)$ is the confluent hypergeometric function [24]. In addition, G_1 for all integer values of m is given as follows:

$$G_1 = \frac{2^{m-1}(m-1)!}{\left(\frac{m}{\overline{\gamma_j}}\right)^m}\frac{\overline{\gamma_j}}{m+\overline{\gamma_j}}\exp^{-\frac{\delta}{2}\frac{m}{m+\overline{\gamma_j}}} \times\left[\left(1+\frac{m}{\overline{\gamma_j}}\right)\left(\frac{m}{m+\overline{\gamma_j}}\right)^{m-1}L_{m-1}\left(-\frac{\delta}{2}\frac{\overline{\gamma_j}}{m+\overline{\gamma_j}}\right) + \sum_{n=0}^{m-2}\left(\frac{m}{m+\overline{\gamma_j}}\right)^n L_n\left(-\frac{\delta}{2}\frac{\overline{\gamma_j}}{m+\overline{\gamma_j}}\right)\right]. \tag{14}$$

Similar to the AWGN scenario, the average probabilities of misdetection and false alarm are obtained using (6) and (7).

C. Energy Cost of Sensing

One of the important concerns in the design of the CRNs is the energy cost of the spectrum sensing because it is a major contributor to the total energy consumption. Suppose the energy cost of sensing one channel by an SU is E_S and the energy costs associated with reporting the sensing results are E_{TX} (corresponding to transmitter energy consumption at the SU) and E_{RX} (corresponding to receiver energy consumption at the BS). The energy costs associated with BS informing an SU of the channel to sense in the next frame are E_{TX} for the BS and E_{RX} for the SU. In addition, the energy cost of idling during T_S is E_{id}.

The energy costs associated to sensing depending on whether or not an SU is assigned to sense a channel are E_1 and E_2, respectively, and are given by

$$E_1 = E_S + 2(E_{\text{TX}} + E_{\text{RX}}) \tag{15a}$$

$$E_2 = E_{id} + E_{\text{TX}} + E_{\text{RX}}. \tag{15b}$$

In (15a), an SU has to report its sensing results to the BS and consequently the BS sends SU the information about the sensing assignments for the time frame. Hence, the cost of communication with the BS ($E_{\text{TX}} + E_{\text{RX}}$) is included twice.

In comparison, the energy cost of spectrum sensing in the greedy noncooperative policy [28] E_t^g is obtained as $E_t^g = E_S + E_{\text{TX}} + E_{\text{RX}}$, noting that all the SUs independently choose to sense the best possible channel and transmit the outcome of sensing that channel to the BS. Similarly, the energy cost of spectrum sensing in the genie-aided spectrum sensing policy E_t^{ga} is obtained as $E_t^{\text{ga}} = \text{M}\,\text{E}_S + E_{\text{TX}} + E_{\text{RX}}$. In this case, all the SUs sense the entire spectrum band and transmit the results to the BS. In our numerical simulations, we compare energy cost of our proposed policy with these two policies assuming the cost of accessing an empty channel is equal to E_{acc} for all three policies. The energy cost per successful SU channel access is the sum of average energy cost to find an empty channel plus the cost to access a channel (i.e., E_{acc}).

VI. Numerical Results

For our numerical simulations, we set $N = 50$, $M = 10$, and $N_p = 20$ and assume that SUs are distributed uniformly at random in an area with size $A = 1000^2$ (distance unit)^2. At this

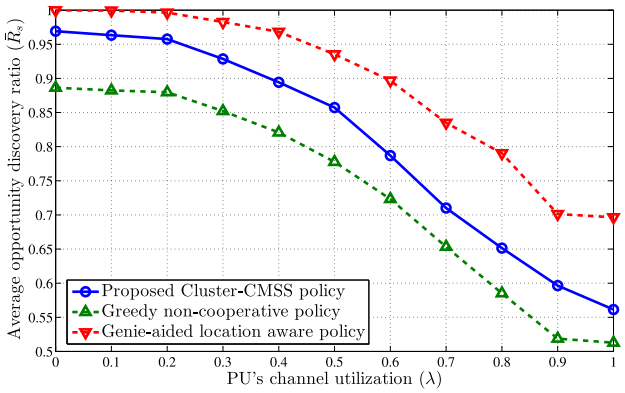

Fig. 4. Average spectrum opportunity discovery ratio versus the PU's channel utilization λ.

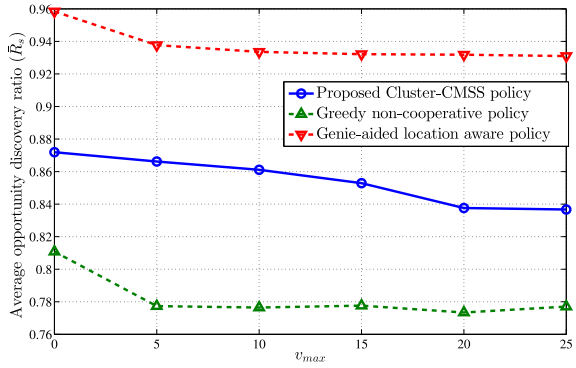

Fig. 5. Average spectrum opportunity discovery ratio versus maximum velocity of SU's movement ($v_{\max}$).

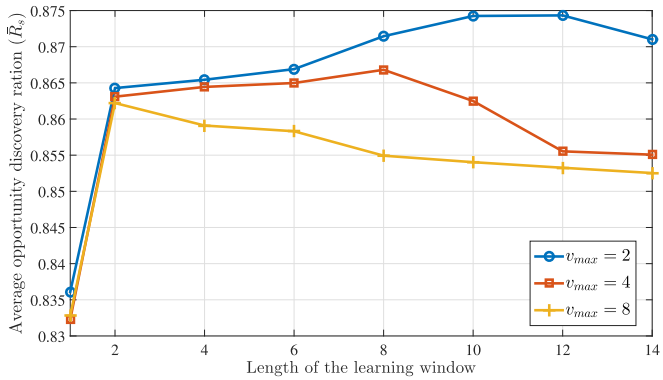

Fig. 6. Average spectrum opportunity discovery ratio versus the length of the learning window.

point, for all PUs, we assume the AWGN channel scenario and the received signal power is only affected by path loss with path loss exponent $\gamma = 2.7$. We suppose SUs can detect each PU's transmission within 100 distance unit range with a high probability. For the brevity of the results, we assume the channels for all PUs have similar parameters (i.e., $\alpha_{l,i} = \alpha$, $\beta_{l,i} = \beta$, and $\lambda_{l,i} = \lambda$ for all $i = 1, \ldots, M$ and $l = 1, \ldots, N_p$). We set $\alpha = 0.1$ and change the value of β to obtain the desired channel utilization λ. For cluster-CMSS, the number of clusters is determined using the elbow method described in Section IV-C. The results of this simulation is shown in Fig. 4, which represents the *average spectrum opportunity discovery ratio* ($\bar{R}_s$), as defined in (2), versus λ. In addition, the SUs move according to the random waypoint model RWP$(0, 15, 2.5)$.

In Fig. 4, we compare the spectrum sensing performance of our proposed cluster-CMSS policy with a genie-aided location aware policy and the greedy noncooperative spectrum sensing policy in [28]. In the genie-aided sensing policy, the BS is aware of the status of the previous channel states at all SUs and the distance between SUs. Clearly implementing the genie-aided policy in a geographically dispersed and mobile network is impractical. Therefore, the genie-aided policy solely serves as a performance upper bound. As we can see, when PU channels are underutilized, all policies have a high opportunity discovery rate due to abundance of spectrum holes. However, when λ is close to 1 (heavy PU utilization), our proposed policy performs better than the greedy noncooperative policy by at least 15%. By increasing the channel utilization, the spectrum holes become more scarce and the effectiveness of the proposed policy in finding spectrum holes becomes more lucid.

In Fig. 5, we have depicted the average opportunity discovery ratio of cluster-CMSS versus the maximum velocity of the SU in the random waypoint model. We set the same parameters as previous simulation ($N = 50$, $M = 10$, $N_p = 20$, $\lambda = 0.5$, and $\gamma = 2.7$). The mobility model in this simulation is RWP$(0, v_{\max}, 2.5)$. As we can see, the average opportunity discovery ratio decreases by increasing $v_{\max}$. According to (4), by increasing $v_{\max}$, the length of the learning window decreases. Smaller learning window reduces BS's capability to learn the dynamic behavior of the PU network. Hence, cluster-CMSS will not be able to effectively employ the information from previous channel occupancy of PUs.

In the next simulation, we investigate the effectiveness of the proposed learning window based analysis. Similar to previous simulations, we consider the following parameters for the simulation: $N = 50$, $M = 10$, $N_p = 20$, $\lambda = 0.5$, and $\gamma = 2.7$. We consider different mobility scenarios and different value of $v_{\max}$. In Fig. 6, we depicted the average spectrum opportunity discovery ratio versus the length of the learning window. As opposed to previous simulations in which we found the length of learning window from (4) of Theorem 1, in this simulation we obtained $\bar{R}_s$ versus different lengths of the learning window. As we can see in Fig. 6, the maximum opportunity discovery ratio for different $v_{\max}$ values occurs at the length of the learning window that is predicted by (4). This figure verifies the results of Theorem 1. For instance at $v_{\max} = 4$, we find $T_l = 8$ using (4). This coincides with the length of the learning window that maximizes the performance in Fig. 6.

In Fig. 7, we represent the numerically-obtained characteristic graph (the probability of misdetection versus the probability of false alarm) of cluster-CMSS and the noncooperative policy in [28], under AWGN, Nakagami–Rician, and Rayleigh channels, assuming the average received SNR is 15 dB. In this simulation, we employ the same simulation parameters as in the previous experiment. We set $K = 10$ and $m = 10$ for the cases of

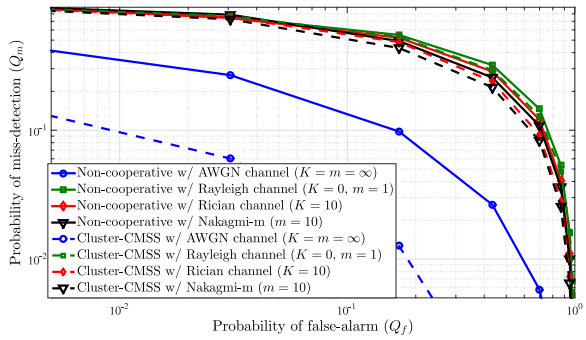

Fig. 7. Numerically obtained characteristic graph of the proposed cluster-CMSS policy and the noncooperative greedy policy in [28] at 15 dB average received SNR.

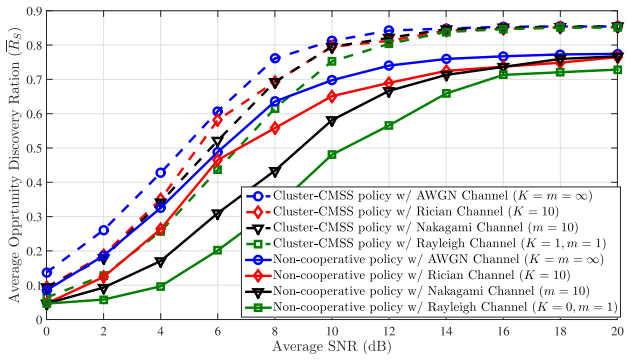

(a)

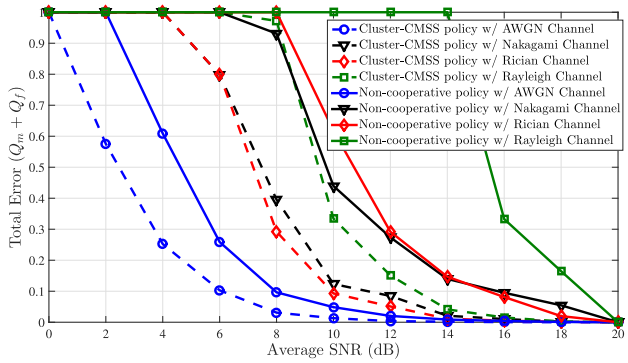

(b)

Fig. 8. Performance of the proposed cluster-CMSS versus SNR under different channel fading models. (a) Opportunity discovery ratio versus the average received SNR for different fading models. (b) Total error ($Q_m + Q_f$) versus the average received SNR for different models.

Rician fading and Nakagami fading, respectively. As we can see, cluster-CMSS has a better performance under all channel conditions compared to the noncooperative policy [28]. Moreover, cluster-CMSS is the most effective in the AWGN scenario. As expected Rayleigh channel model has the worst performance due to the more severe fading condition.

In the next simulation, we compare the performance of our proposed cluster CMSS algorithm with the noncooperative scenario under different channel fading models. Since the cluster-CMSS algorithm has been developed under the assumption of ideal sensing, it is imperative to show that it will work well under nonideal cases as well. In Fig. 8(a), we depicted the average opportunity discovery ratio versus the received average SNR (in dB) for AWGN, Rician (with $K = 10$), Nakagami ($m = 10$), and Rayleigh fading models. In Fig. 8(b), for the same channel fading models, we have depicted the total error ($Q_m + Q_f$) versus the average received SNR (in decibels). In Fig. 8 the simulation parameters are $N = 50$, $M = 10$, $N_p = 20$, $\lambda = 0.5$, and RWP$(0, 15, 2.5)$. As we can see the proposed cluster-CMSS performs better than noncooperative scenario for both low-SNR and high-SNR regimes for all the channel fading models.

TABLE I
AVERAGE ENERGY COST PER SUCCESSFUL SU TRANSMISSION

Spectrum sensing policy	Energy cost (mJ)
Cluster-CMSS	7.97
Greedy noncooperative	7.725
Genie-aided	39.22

Now, let us pair cluster-CMSS with a very simple spectrum access scheme (described in Section V-C), which basically allows every SU to access the channel it finds empty and transmit on that channel. The simulation parameters are similar to previous simulations (i.e., $N = 50$, $M = 10$, $N_p = 20$, $\lambda = 0.5$, and $\gamma = 2.7$). In Table I, we compare the average energy costs per successful SU transmission in one time frame for different policies. As reported in [29], the energy cost of an SU to sense one channel, to transmit/receive a channel sensing result, to access a channel, and to idle during sensing time is $E_S = 3.5$ mJ, $E_{\text{TX}} = E_{\text{RX}} = 0.1125$ mJ, $E_{\text{acc}} = 4$ mJ, and $E_{\text{id}} = 0.05$ mJ, respectively. Therefore, we find the energy cost of different policies using the simple access scheme (every SU accesses the channel it finds empty).

As it can be concluded from Table I, the energy cost of cluster-CMSS is slightly higher, because of coordination overhead, than noncooperative greedy policy. This slight increase in energy consumption is the price of larger opportunity discovery ratio in the spectrum sensing. In addition, we have included the energy cost that is required to implement the genie-aided policy, which is considerably larger than our proposed cluster-CMSS and greedy policies.

VII. CONCLUSION

In this paper, we considered the problem of CMSS in the geographically disperse and mobile CRNs. We proposed a policy that detects the spectrum holes without depending on the location information of the PUs. According to our proposed policy, the SUs are clustered based on their spectrum sensing results. We introduced a novel metric for clustering SU nodes, which is based on the consensus among the SUs' channel sensing results. In our proposed policy, the BS uses this metric to form the clusters without the need to know the location of the SUs. Then, the BS performs a graph-theory-based coordinated spectrum sensing among members of each cluster. For the mobile SUs that move according to a random waypoint model, we have

shown through extensive simulations that the proposed policy considerably increases the spectrum opportunity discovery ratio for the SUs at the cost of a slight increase in the energy consumption associated with spectrum sensing.

APPENDIX

To prove Theorem 1, assume an SU is located inside a circle with radius R; we want to find the average amount of time that it takes for the SU to leave that circle. The mobility model is RWP$(v_{\min}, v_{\max}, t_p)$. Hence, the SU will leave the circle if its new waypoint lies outside the circle with radius R. Let P_{in} be the probability that a waypoint is chosen inside the circle with radius R and is denoted by $P_{\text{in}} = \frac{\pi R^2}{A}$. The number of epochs that the SU takes to leave the circle follows a geometric distribution with success probability $1 - P_{\text{in}}$. Accordingly, on average it will take $\frac{P_{\text{in}}}{1-P_{\text{in}}}$ epochs before it leaves the circle. Given that waypoint is located inside the circle. The average time of an epoch with a waypoint inside the circle R is T_{in} and is obtained as follows:

$$T_{\text{in}} = \frac{\frac{128R}{45\pi}}{\frac{v_{\min}+v_{\max}}{2}} + t_p. \tag{16}$$

In (16), the numerator is the average distance between any two points in a circle with radius R chosen uniformly at random [30] and the denominator is the average velocity. On the other hand, given that the waypoint falls outside of the circle, it will take T_{edge} seconds on average until it reaches the edge of the circle and leaves it. Accordingly T_{edge} is determined by finding the average distance of random point inside a circle to any point in its circumference and dividing it to the average speed. Within a circle with radius R is located at the origin, the average distance of a point at location $(r, 0)$ to any point in its circumference is obtained as follows:

$$\begin{aligned} L_{\text{edge}}(r) &= \frac{1}{2\pi}\int_0^{2\pi} \sqrt{(R\cos\phi - r)^2 + R^2\sin^2\phi}\, d\phi \\ &= \frac{2}{\pi}\left|1 - \frac{r}{R}\right| E_e\left(-\frac{4r/R}{(1-r/R)^2}\right) \end{aligned} \tag{17}$$

where $E_e(r)$ is the complete elliptical integral of the second kind, which is defined as $E_e(r) \triangleq \int_0^{\frac{\pi}{2}} \sqrt{1 - r^2\sin^2(\theta)}\, d\theta$. It is easy to verify that for all $0 \le \frac{r}{R} \le 1$, we have $1 \le \frac{2}{\pi}|1 - \frac{r}{R}|E_e(-\frac{4r/R}{(1-r/R)^2}) \le \frac{4}{3}$. Therefore, $1 \le L_{\text{edge}} \le \frac{4}{3}$.

Accordingly, we obtain T_{edge} as follows:

$$T_{\text{edge}}(r) = \frac{L_{\text{edge}}}{\frac{v_{\min}+v_{\max}}{2}} = \frac{\frac{4}{\pi}|1 - \frac{r}{R}|}{v_{\min} + v_{\max}} E_e\left(-\frac{4r/R}{(1-r/R)^2}\right). \tag{18}$$

Accordingly, the average time an SU takes to move out of the range of a PU is

$$T_r = \frac{P_{\text{in}}}{1 - P_{\text{in}}} T_{\text{in}} + T_{\text{edge}} \tag{19}$$

The upper bound and the lower bound on (19) is obtained as follows:

$$\begin{aligned} &\frac{2}{v_{\min} + v_{\max}}\left(\frac{P_{\text{in}}}{1 - P_{\text{in}}}\frac{128R}{45\pi} + 1\right) + \frac{P_{\text{in}}}{1 - P_{\text{in}}} t_p \le T_r \\ &\le \frac{2}{(v_{\min} + v_{\max})}\left(\frac{P_{\text{in}}}{1 - P_{\text{in}}}\frac{128R}{45\pi} + \frac{4}{3}\right) + \frac{P_{\text{in}}}{1 - P_{\text{in}}} t_p. \end{aligned} \tag{20}$$

REFERENCES

[1] I. F. Akyildiz, W.-Y. Lee, M. C. Vuran, and S. Mohanty, "Next generation/dynamic spectrum access/cognitive radio wireless networks: A survey," *Comput. Netw.*, vol. 50, no. 13, pp. 2127–2159, May 2006.

[2] S. Haykin, "Cognitive radio: Brain-empowered wireless communications," *IEEE J. Select. Areas Commun.*, vol. 23, no. 2, pp. 201–220, Feb. 2005.

[3] I. F. Akyildiz, B. F. Lo, and R. Balakrishnan, "Cooperative spectrum sensing in cognitive radio networks: A survey," *Phys. Commun.*, vol. 4, no. 1, pp. 40–62, Dec. 2011. [Online]. Available: http://www.sciencedirect.com/science/article/pii/S187449071000039X

[4] W.-Y. Lee and I. Akyildiz, "Optimal spectrum sensing framework for cognitive radio networks," *IEEE Trans. Wireless Commun.*, vol. 7, no. 10, pp. 3845–3857, Oct. 2008.

[5] T. Do and B. Mark, "Joint spatial-temporal spectrum sensing for cognitive radio networks," *IEEE Trans. Veh. Technol.*, vol. 59, no. 7, pp. 3480–3490, Sep. 2010.

[6] Q. Wu, G. Ding, J. Wang, and Y.-D. Yao, "Spatial-temporal opportunity detection for spectrum-heterogeneous cognitive radio networks: Two-dimensional sensing," *IEEE Trans. Wireless Commun.*, vol. 12, no. 2, pp. 516–526, Feb. 2013.

[7] Z. Quan, S. Cui, A. Sayed, and H. Poor, "Optimal multiband joint detection for spectrum sensing in cognitive radio networks," *IEEE Trans. Signal Process.*, vol. 57, no. 3, pp. 1128–1140, Mar. 2009.

[8] A. Singh, M. R. Bhatnagar, and R. K. Mallik, "Performance of an improved energy detector in multihop cognitive radio networks," *IEEE Trans. Veh. Technol.*, vol. 65, no. 2, pp. 732–743, Feb. 2016.

[9] H. Liu, K. Liu, and Q. Zhao, "Learning in a changing world: Restless multiarmed bandit with unknown dynamics," *IEEE Trans. Inf. Theory*, vol. 59, no. 3, pp. 1902–1916, Mar. 2013.

[10] Z. Wang, Z. Feng, and P. Zhang, "An iterative Hungarian algorithm based coordinated spectrum sensing strategy," *IEEE Commun. Lett.*, vol. 15, no. 1, pp. 49–51, Jan. 2011.

[11] J. Oksanen, J. Lundén, and V. Koivunen, "Reinforcement learning based sensing policy optimization for energy efficient cognitive radio networks," *Neurocomputing*, vol. 80, pp. 102–110, Mar. 2012.

[12] A. W. Min and K. G. Shin, "Impact of mobility on spectrum sensing in cognitive radio networks," in *Proc. ACM Workshop Cogn. Radio Netw.*, Beijing, China: ACM, no. 6, pp. 13–18, Sep. 2009, doi: 10.1145/1614235.1614239.

[13] W. Ren, Q. Zhao, and A. Swami, "Temporal traffic dynamics improve the connectivity of ad hoc cognitive radio networks," *IEEE/ACM Trans. Netw.*, vol. 22, no. 1, pp. 124–136, Feb. 2014. [Online]. Available: http://dx.doi.org/10.1109/TNET.2013.2244612

[14] G. Caso, H. Soleimani, L. De Nardis, A. Tosti, and M. Di Benedetto, "SENSIC: Mobility-aware cluster-based cooperative spectrum sensing for cognitive radio networks," in *Proc. IEEE Int. Conf. Ultra-WideBand*, Sep. 2014, pp. 102–107.

[15] B. Shahrasbi and N. Rahnavard, "A clustering-based coordinated spectrum sensing in wideband large-scale cognitive radio networks," in *Proc. IEEE Global Commun. Conf.*, Dec. 2013, pp. 1101–1106.

[16] M. Bradonjic and L. Lazos, "Graph-based criteria for spectrum-aware clustering in cognitive radio networks," *Ad Hoc Netw.*, vol. 10, no. 1, pp. 75–94, Jan. 2012.

[17] Y. Liu, S. Xie, R. Yu, Y. Zhang, and C. Yuen, "An efficient MAC protocol with selective grouping and cooperative sensing in cognitive radio networks," *IEEE Trans. Veh. Technol.*, vol. 62, no. 8, pp. 3928–3941, Oct. 2013.

[18] S. Liu, I. Ahmad, Y. Bai, Z. Feng, Q. Zhang, and Y. Zhang, "A novel cooperative sensing based on spatial distance and reliability clustering scheme in cognitive radio system," in *Proc. IEEE 78th Veh. Technol. Conf.*, Sep. 2013, pp. 1–5.

[19] Y. Sun, H. Hu, F. Liu, H. Yi, and X. Wang, "Selection of sensing nodes in cognitive radio system based on correlation of sensing information," in *Proc. 4th Int. Conf. Wireless Commun., Netw. Mobile Comput.*, Oct. 2008, pp. 1–6.
[20] H. Kim and K. Shin, "Efficient discovery of spectrum opportunities with MAC-layer sensing in cognitive radio networks," *IEEE Trans. Mobile Comput.*, vol. 7, no. 5, pp. 533–545, May 2008.
[21] W. Dai, Y. Gai, and B. Krishnamachari, "Online learning for multi-channel opportunistic access over unknown markovian channels," in *Proc. 11th Annu. IEEE Int. Conf. Sens., Commun. Netw.,* Jun. 2014, pp. 64–71.
[22] R. Tibshirani, G. Walther, and T. Hastie, "Estimating the number of clusters in a data set via the gap statistic," *J. Roy. Statist. Soc., Ser. B (Statisti. Methodol.)*, vol. 63, no. 2, pp. 411–423, 2001. [Online]. Available: http://dx.doi.org/10.1111/1467-9868.00293
[23] R. Diestel, *Graph Theory* (Graduate Texts in Mathematics). Berlin, Germany: Springer, 2005, vol. 91, p. 92.
[24] F. Digham, M. Alouini, and M. K. Simon, "On the energy detection of unknown signals over fading channels," *IEEE Trans. Commun.*, vol. 55, no. 1, pp. 21–24, May 2007.
[25] A. Abdi, C. Tepedelenlioglu, M. Kaveh, and G. Giannakis, "On the estimation of the *k* parameter for the rice fading distribution," *IEEE Commun. Lett.*, vol. 5, no. 3, pp. 92–94, Mar. 2001.
[26] A. Goldsmith, *Wireless Communications*. Cambridge, U.K.: Cambridge Univ. Press, 2005.
[27] N. Beaulieu and C. Cheng, "Efficient Nakagami-m fading channel simulation," *IEEE Trans. Veh. Technol.*, vol. 54, no. 2, pp. 413–424, Mar. 2005.
[28] C. Tekin, S. Hong, and W. Stark, "Enhancing cognitive radio dynamic spectrum sensing through adaptive learning," in *Proc. IEEE Mil. Commun. Conf.,*, Oct. 2009, pp. 1–7.
[29] D. Xue, E. Ekici, and M. C. Vuran, "CORN2: Correlation-based cooperative spectrum sensing in cognitive radio networks," in *Proc. 10th Int. Symp. Modeling Optimization Mobile, Ad Hoc Wireless Netw.,*, May 2012.
[30] R. García-Pelayo, "Distribution of distance in the spheroid," *J. Phys. A: Math. General*, vol. 38, no. 16, 2005, Art. no. 3475.

Behzad Shahrasbi (S'07–M'16) received the Bachelor's degree from Amirkabir University of Technology, Tehran, Iran; the Master's degree from Oklahoma State University, Stillwater, OK, USA; and the Ph.D. degree from the University of Central Florida, Orlando, FL, USA, in 2006, 2011, and 2015, respectively.

His research interests include sparse signal representations, compressed sensing and recovery algorithms, low rank matrix recovery, and approximation.

Nazanin Rahnavard (S'97–M'10) received the Ph.D. degree from the School of Electrical and Computer Engineering, Georgia Institute of Technology, Atlanta, GA, USA, in 2007.

She is currently an Associate Professor with the Department of Electrical and Computer Engineering, University of Central Florida, Orlando, FL, USA. Her research interests include communications, networking, and signal processing.

Dr. Rahnavard received the National Science Foundation CAREER award in 2011. She serves on the editorial board of the Elsevier *Journal on Computer Networks* and the Technical Program Commitees of several prestigious international conferences.

Azadeh Vosoughi (M'06–SM'14) received the B.S. degree from Sharif University of Technology, Tehran, Iran; the M.S. degree from Worcester Polytechnic Institute, Worcester, MA, USA; and the Ph.D. degree from Cornell University, Ithaca, NY, USA, in 1997, 2001, and 2006, respectively, all in electrical engineering.

She is currently an Associate Professor with the Department of Electrical Engineering and Computer Science, University of Central Florida, Orlando, FL, USA. Her research interests include wireless communications, statistical signal processing, distributed detection and estimation theory, and brain signal processing.

Dr. Vosoughi received the National Science Foundation CAREER award in 2011. She is currently an Associate Editor for the IEEE SIGNAL PROCESSING LETTERS.